

# SSF3D: Strict Semi-Supervised 3D Object Detection with Switching Filter

1<sup>st</sup> Songbur Wong

School of Aeronautics and Astronautics, SJTU

ShangHai, China

songbur\_929@sjtu.edu.cn

**Abstract**—SSF3D modified the semi-supervised 3D object detection (SS3DOD) framework, which designed specifically for point cloud data. Leveraging the characteristics of non-coincidence and weak correlation of target objects in point cloud, we adopt a strategy of retaining only the truth-determining pseudo labels and trimming the other fuzzy labels with points, instead of pursuing a balance between the quantity and quality of pseudo labels. Besides, we notice that changing the filter will make the model meet different distributed targets, which is beneficial to break the training bottleneck. Two mechanism are introduced to achieve above ideas: strict threshold and filter switching. The experiments are conducted to analyze the effectiveness of above approaches and their impact on the overall performance of the system. Evaluating on the KITTI dataset, SSF3D exhibits superior performance compared to the current state-of-the-art methods. The code will be released here.

## I. INTRODUCTION

In 3D object detection from LIDAR point clouds, supervised deep learning methods currently dominate. These approaches require extensive human effort for annotation, training and optimization on different scenes, limiting their generalization capability. Semi-supervised learning using teacher-student method [1] alleviated this problem by utilizing pseudo labels generated from teacher models. Over the past few years, this system has been extensively explored and shown great model enhancement capabilities [2]. This paper focus on the semi-supervised learning with teacher-student approach, in particular for 3d object detection(3DOD) with LIDAR point clouds.

For SS3DOD, the teacher-student framework is used as one of the most widely proven semi-supervised learning method. Key idea of this system is to create a performance gap between teacher and student models by applying different augmentations, then use the teacher’s outputs as pseudo-labels to supervise the student training, which allows exploiting abundant unlabeled data. During the training, student model’s parameters keep updating, while the teacher’s parameters are renew from student’s by exponential moving average (EMA) strategy commonly. Recently, the SS3DOD system pioneered by 3DIOUMatch [19] has led to some works [13], [18], [25], these methods have proposed operators for refining teachers’ prediction boxes, while in these filtering processes, there still exists a question: the retention of erroneous targets generated from teacher network leads to interference with training. There

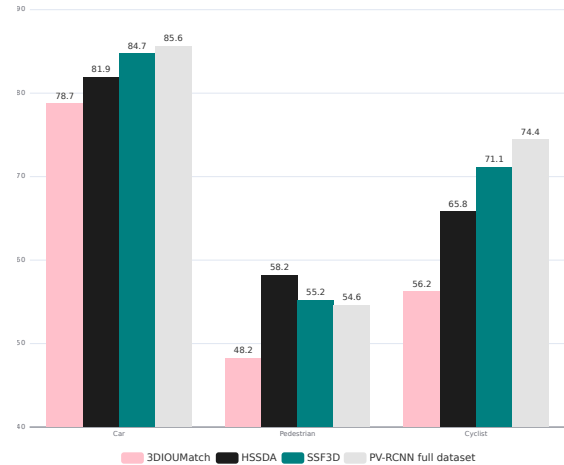


Fig. 1. The proposed SSF3D result compare with state-of-the-art SS3DOD algorithms [13], [19] using only 2% labeled KITTI [32] data, and full-dataset supervised result is given in gray bars.

are two main reasons for this problem, as shown in the Fig. 2 and Fig 3.

One is that the current method adopts an imprecise design in the selection of filter threshold in order to balance the number and accuracy of retained labels. Another is the current filters that rely solely on model confidence scores will classify some targets with less information into labels, those low information targets are sometimes have same points distribution with other artificial objects, which tend to be harmful to models training, especially for lightweight ones.

To address the limitation mentioned, we propose a strict teacher-student system with switching filters in different stages called SSF3D. Following prior works, SSF3D adopts a point remove operation - eliminating the filtered box along with the points inside the box, due to the existence of this operation, in the tradeoff between the precision and the number of labels, it’s possible to avoid penalty of the model being affected by false negative labels while improving the accuracy of the retained labels as much as possible. Specifically, we renew the threshold selection method to restrict the pseudo-labels to high-confidence boxes, meanwhile use the Quality Focal Loss [16] for suppressing the effects of possible false negative labels. With the help these tricks, the student model will

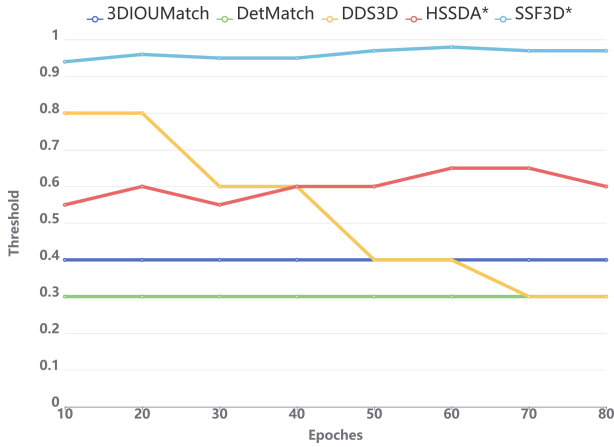


Fig. 2. **Threshold picking of different methods.** The confidence thresholds selected by different SS3DOD methods in recent years [13], [18], [19], [25] are listed here, noted that those value are for car class, and means the lowest predictive score of the boxes that will be retained as labels. It can be seen that except our method, all other architecture adopt a moderate threshold to make a tradeoff between label quantity and quality, meanwhile introduce some incorrect labels. The \* methods uses a point remove strategy.

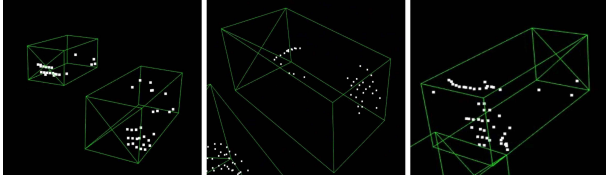


Fig. 3. **Ambiguous pseudo labels retained by confidence filters.** In previous works, some ambiguous targets that have same points distribution with sundries are remained.

only see the points within the high-confidence labels and background points during training.

Another attempt to improve the quality of pseudo labels is to switch the filtering strategy in different stages of training. As shown in Fig. 3, some targets are regard as labels but it is evident that these goals are indistinguishable even with the human eyes. We believe that this case is caused by the feature distribution similarity, which means these ambiguous targets have similar latent feature with the true labels. And in this situation, only use confidence filter for more training is not suitable.

To mitigate this, we propose "Entropy filter" based on normal consistency, which filter calculates the relationship between box and points inside to evaluate the information content of a label and filtering against that standard. By switch on Entropy filter after several epochs of training with confidence filter, the model encounter different true positive labels with different features.

With the above strategies, SSF3D achieves a significant improvement on the KITTI benchmark [32], comparing to the state-of-the-art HSSDA [13]. Using 1%, 2% of labeled data for the car category, SSF3D achieved inference mAP increase of 2.5%, 2.8% respectively under 0.7 IoU at 40 recall. For the smaller target class, cyclist, using only 1% labeled data,

SSF3D achieved a 20% improvement in inference accuracy over previous approaches. This significant gain demonstrates the advantage of SSF3D for few-shot detection.

Our main contributions can be summarized as follows:

- We propose SSF3D, a SS3DOD architecture that is highly compatible with point cloud data. Leveraging the sparse and non-overlapping target distribution in point cloud frames, SSF3D reduced the artificial disturbs introduced in traditional semi-supervised framework.
- Specifically, we select Gaussian Mixture Modeling and Quality Focal Loss as tools to conduct a strict training, and introduce a filter-switching strategy to further enhance label quality. The innovation of strict training and filter-switching strategy from the perspective of threshold and filter design reduces the side effects of false positive labels.
- We achieve notably improved performance over the previous state-of-the-art SS3DOD method on KITTI dataset with 1% and 2% labels, meanwhile two target level point cloud data augmentation methods are used to conduct experiments and perform analysis.

## II. RELATED WORK

### A. 3D Object Detection with LIDAR Point Clouds

For 3DOD with LIDAR point clouds, major data representations include voxel-based [3], [5], [6], [9], [10], [24], [33], [34], point-based [35]–[38], and hybrid voxel-point methods [7], [8], [39]. Architecturally, one-stage [3], [5], [6], [34], [36] and two-stage [7], [8], [38], [40] frameworks exist.

In outdoor scenes, voxel and voxel-point approaches are prevalent since huge raw point sets are computationally expensive. For voxel methods, bird’s eye view (BEV) detection is common. PillarNeXt [6] achieved high accuracy using only pillar voxel features, PV-RCNN [7] exemplifies two-stage techniques - generating proposals in BEV then refining with points. It demonstrated state-of-the-art results at the time by effectively combining both voxel and point features, meanwhile remains a strong competitor in 3DOD.

Currently, self-attention models [41] have become popular in computer vision. For 3DOD, many approaches apply transformers to learn intricate features from point clouds [4], [6], [10], [34]. Transformers excel at capturing complex representations but require abundant labeled datam, while their high capacity also enables generating more accurate pseudo-labels, which facilitates semi-supervised learning. Thus, transformer-based 3DOD models are also well-suited for semi-supervised paradigms.

Generally speaking, a fine designed semi-supervised learning system can benefit most 3D object detection algorithms, and our SSF3D is designed for this purpose. Many pioneering studies have used PV-RCNN [7] as a testbed, so we will also conduct experiments on PV-RCNN to evaluate SSF3D. Thanks to OpenPCDet [42], our semi-supervised methods can be easily applied to various other 3D detection algorithms besides PV-RCNN.

## B. Semi-supervised Object Detection

STAC [21] pioneered teacher-student frameworks for 2D semi-supervised object detection (SSOD), using offline training. After that several approaches have driven progress in semi-supervised 2D object detection. Unbiased Teacher [20] introduced end-to-end training and difference augmentation strategies. Soft Teacher [15] decoupled the prediction heads and proposed box jittering to refine pseudo-labels. Unbiased Teacher v2 [30] introduced a Listen2Student mechanism that filtered regression labels by uncertainty to enable anchor-free models. Dense Teacher [16] weighted pseudo-box loss based on model confidence scores, and consistent Teacher [14] prevented label drift via insert a short branch to calibrate the predict labels use the classification scores.

The extensive research and experience with 2D data has been leveraged by researchers to be applied to 3D domains, 3DIOUMatch [19] set a milestone in SS3DOD, they create an IOU with detect-score guided filter for pseudo labels. SE-SSD [23] used a mixup-like [28] technique to combine and mix the point clouds of different objects during training, meanwhile refined the training loss which brings great benefit. Dynamic threshold and dense pseudo labels are utilized in DDS3D [18] to generate more correct labels, which enhances the model’s performance. However, these operations have some drawbacks during training as they introduce artificially negative pseudo labels and can lead to ambiguity in the training process. DetMatch [25] use a two-teacher system to leverage 2D information to boost the SS3DOD, which improved the quality of the model but new training complexity is introduced. HSSDA [13] integrates previous works and proposed a complete offline - online semi-supervised learning architecture.

Above works meanly inherit the 2D semi-supervised learning thought that the effect of false negative labels is inevitable, so the filtering idea of labels is also eclectic to give a better tradeoff. While in SSF3D, strict filter mechanism replaces the previous eclectic, all the points possible lead to ambiguous are removed, meanwhile we add a filter switching strategy to further optimize the pseudo labels. It’s proved that in small dataset as KITTI, this strategy can bring a significant improvement. In relation to previous works, we leverage HSSDA’s architecture and re-designed the filter mechanism, the specific framework will be given in Sec. III-A.

## III. METHOD

### A. Overall Framework

SSF3D inherit online-offline alternating training framework from [13], which means teacher model not only generate pseudo labels during training, but also save the high scoring boxes with points offline for the convenience of gt augmentation [24]. the specific framework is shown in Algorithm 1.

In this framework, GMM3 threshold picking method, Dense Loss and Entropy-filter with a switching filter strategy are designs we introduced, and will be specifically interpreted in Sec. III-B1, Sec. III-B2 and Sec. III-C.

---

### Algorithm 1: PyTorch-style pseudo code of SSF3D framework.

---

```
# d: the whole dataset with unlabeled data.
# d_l: part of the dataset that is labeled.
# m_t, m_s: teacher and studnet model.
# GMM3: threshold picking method.
# Filter: label filter method, include 3
#       sub-filters for two-stage prediction scores and a
#       custom filter score.
# dense_l, reg_l: classification loss and
#       regression loss for SSF3D.
# remove_pts(d, reslut): functions that remove low
#       score result covered points from data.
# m: momentum.
# gt_aug: random add saved pseudo label into each
#       frame.
m_t, m_s = pretrain_model # initialize.
m_t.detach()
Filter = iou_filter # initialize filter.
for epoch in total_epochs:
    if epoch > set_epoch:
        Filter = entropy_filter
        # switch filter after several epoches.

    if epoch // freq == 0: # threshold and local
        label updated every freq epoches.
        x_1 = m_t(d_l), thr = GMM3(x_1)
        x_2 = m_t(d)
        pseudo_label = Filter(x_2, thr)
        d.update(pseudo_label) # save the pseudo
        labels in dataset for future training.

    d_temp = gt_aug(d)
    y_1 = m_t(d_temp)
    disposable_label = Filter(y_1, thr)
    # generate single-use label for each epoch
    label = concat(d_temp[label], disposable_label)
    d_temp = remove_pts(d_temp, y_1)
    y_2 = m_s(d_temp)

    loss = dense_l(label, y) + reg_l(label, y)
    loss.backward()
    # In the actual calculation, the iteration is
    carried out in batch
    update(m_s.params)
    m_t.params = m * m_t.params + (1 - m) * m_s.params
```

---

### B. Strict Mechanism

Strict Mechanism is a key factor make the SSF3D surpass other algorithms. Following previous work, combination of delete and add is used in SSF3D. Delete means we remove all points from the box whose detective score does not exceed the filter threshold, in each frame. Add means we save the boxes with points that pass the filter, then randomly add them

into different scene as gt augmentation [24]. Delete operation makes student model won't generate loss on ambiguous targets, which help this framework more robust to the false negative labels. While add operation ensures the model can reach enough targets to learn.

Therefore, threshold that can determine whether a set of target points is deleted or added becomes the key to the design, to remain true positive pseudo label as correct as possible, the threshold need to be strict but not extreme. So we design GMM3 Picker to find this threshold. Simultaneously, we reference Dense Loss [16] to maintain the pseudo label's quality during generate single-use label for each epoch, these two methods work together to ensure a more stringent label filtering than previous works.

1) *GMM3 Picker*: GMM3 Picker attempt to select suitable thresholds automatically from data with true labels. As mentioned in Algorithm 1, all boxes detected on the labeled partial dataset and their corresponding scores will be recorded, each boxes commonly related to three scores: two scores from two-stage detection, and one score from the custom filter.

Suppose there are  $n$  targets in partial dataset with label information, and the teacher model contains  $m$  detection results for this dataset. Then calculate the intersection over union (IOU) between  $n$  targets and  $m$  detection results, pick the IOU greater than a baseline  $bs\_line=0.5$  from detection results as the positive samples. If there are  $l$  ( $l \leq m \cap n$ ) positive samples, then there will be a  $(l \times 3)$  tensor that record the three scores, we put each  $l$  scores into a 3-level Gaussian Mixture Modeling (GMM)  $P(s)$  to search the correct threshold, which can be described as

$$P(s) = \sum_{k=1}^3 \omega_k \mathcal{N}(s | \mu_k, \Sigma_k), \quad \sum_{k=1}^3 \omega_k = 1, \quad (1)$$

where  $\mathcal{N}(s | \mu_k, \Sigma_k)$  represent a distribution of each level threshold, and  $\omega_k, \mu_k, \Sigma_k$  denote the weight, mean and variance of each level threshold, the mean of each level will be calculated from an Expectation-Maximization (EM) algorithm, after GMM fitting, we generate 3 thresholds from each  $l$  scores, and for a strict filter, we choose the high or middle threshold as the final threshold. In the end, 3 thresholds will be used to filter the pseudo labels, results from teacher model which passed all three thresholds will be set as the final pseudo label.

GMM method can find means of different distributions of the scores, in our case, there are three means, the lowest one is used to filter the noise, specifically, during the selection of positive samples, some boxes with low scores will be selected, and these boxes' scores are likely to be noise. The middle one can be seen as a moderate threshold, this value is enough high in almost situation but sometimes fluctuation by input data. While the highest one mean can generate stable strict threshold, both moderate and strict threshold are used in SSF3D, commonly, the strict threshold is used for confident threshold, and the moderate threshold is used for the threshold of roi score and custom filter.

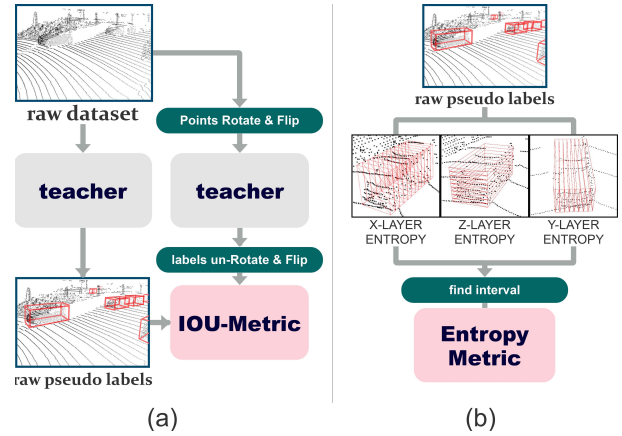


Fig. 4. **Custom filter in 2 stages**. Pipeline of the label filter in SSF3D. in stage-1 training, IOU Filter [13] as Fig. 4 (a) is used. In stage-2 we offline count all prediction boxes' 3-dimension-entropy as Fig. 4 (b) and use the scatterplot of entropy to find a correct range to filter the generated labels.

2) *Dense Loss*: Not only focus on selection of pseudo label, we also borrow the dense loss function [16] to suppress noise labels. After point remove operation, there still have possibility that some ambiguity points exist in the frame, those points have similar feature with the true labels, but didn't be detected by the teacher model, so didn't be removed from the frame. In this case, once student model recognize these points as labels, it will harm to the training process. To avoid this situation, the easy solution is to suppress the effect of low score boxes during training, while dense loss naturally suitable to complete this mission.

We selected dense pseudo loss [16] as the classification loss for two stages of PV-RCNN, which can write as:

$$\mathcal{L}^{\text{cls}} = -|\hat{y} - y_s|^\gamma * [\hat{y} \log y_s + (1 - \hat{y}) \log (1 - y_s)], \quad (2)$$

where  $y_s$  is the predict score of student model, and  $\hat{y}$  obey the following rules in our model:

$$\hat{y} = \begin{cases} y_t, & \text{if } y_t > \tau_{\text{pred}} \ \& \ y_t > \tau_{\text{roi}} \ \& \ y_t > \tau_{\text{thr}} , \\ 0, & \text{otherwise} , \end{cases} \quad (3)$$

where  $y_t$  is the predict score of teacher model,  $\tau_{\text{pred}}$ ,  $\tau_{\text{roi}}$ ,  $\tau_{\text{thr}}$  are thresholds of prediction score, roi score and man-designer filter score.

In situation claired above,  $y_t$  is 0, while the ambiguous target accidentally found have a low value of  $y_s$ , so the nonlinear term  $|\hat{y} - y_s|^\gamma$  can directly suppress these point disturb the training.

Combine GMM3 Picker and Dense Loss, strict mechanism in SSF3D let model only focus on the true positive labels, equivalent to cleaning the data at the same time of end-to-end iterative calculation.

### C. Entropy Filter

Each pseudo label have three scores, two scores from two-stage detection, and one score from the custom filter. The custom filter is also one of the key elements that discriminate

a fine-designed SS3DOD from a vanilla one. We found that with classical filter, which use confidence scores as metrics can't distinguish some targets, those targets seems have similar latent feature with the true labels but lack of informational complexity as Fig. 3, while these target tend to harm the precision of model, especially lightweight models.

To solve this problem, we propose an unsupervised operator that combines the relationship between points and boxes, further evaluates the likelihood of a 3d box to be an annotation by a simple computation, which we call 3d information entropy. In order to retain the capacity of filters that rely on the model's own judgment while adding the entropy filtering on special targets, we adopt a two-step filtering method, which as well ensure that the two filters will not interfere with each other.

As shown in Fig. 4, first step we use the IOU filter [13] to conduct a classical filtering, then in second step replacing it by the entropy filter. Illustrating in Fig. 4(b), in entropy filter, a predict box is divided into multiple layers according to the spacing  $l$  for one direction, and the points distributed in the same layer are considered co-planar, the ratio of points within layer  $i$  to the total number of points in the box is denoted  $p_i$ , and one dimension entropy can be describe as:

$$\mathcal{E}_{\text{dim}} = - \sum_{i=1}^L p_i \log p_i, \quad (4)$$

where  $L$  is the total layers of the box in one dimension. For different classes, we determine three appropriate thresholds for three dimensions of labels, based on their corresponding entropy distribution scatterplot as shown in Fig. 5(a). The label whose entropy score is lower than the threshold will be filtered out. Selection of these thresholds still need human observation, with some trial and error experiments. To verify the effectiveness of the entropy filter, we plot the scatterplot of all prediction boxes in Fig. 5, each scatter in the frame represent a detection result, in each scatterplot include all targets that model detected from 3769 frames of KITTI dataset.

In Fig. 5(a) and Fig. 5(b), the three axes represent the information entropy scores in three directions: axis X, axis Y and axis Z. And the color of each scatter represent the IOU with groundtruth ( $IOU_{gt}$ ), it can be seen that in Fig. 5(a), the area circled by the red represents a low score area of entropy, and it can be verify in Fig. 5(b) that this area indeed contains a large number of false positive labels. For each class of target, we artificially observe the scatterplot like Fig(a) and choose three low score of entropy as the threshold.

We also plot the relationship between the confidence, roi and entropy score in Fig. 5(c), the x,y axis are two scores of prediction and the z-axis is the entropy score of x direction, it can be seen that few targets maintain very low entropy when the detection score is high, and the low entropy targets even in high detection score area,  $IOU_{gt}$  is still not high enough to be a label.

In traditional 3D encoders [43]–[45], the proximity point is used as a unit to compute the normal and encode the point by the relationship between the 3d point normals, whereas

our layer-wise computation also equivalent to measuring the difference between the normals of the points inside the box and the normals of the box boundaries, further estimating the accuracy of the regression box. Compare to traditional encoders, information entropy computation is more specialize in low-level, introduces more prior information and aims to filter out a specific portion of the low-information box, such as some of the walls that have been misdiagnosed as vehicles and so on.

## IV. EXPERIMENTS

### A. Experiments Setups

**Datasets and Evaluation Metrics.** Following the methods raised recent years [13], [18], [19], [25], we use KITTI 3D bench mark [32] as dataset and PV-RCNN as test bed, there are 7481 outdoor scenes for training and 7518 for testing, the training 7481 frames have annotations and is generally used in LiDAR algorithm develop, follow lots of prior researches, we use the divided *train* split of 3,712 samples and *val* split of 3,769 samples as a common practice. Using the released 3D IoU match [19] splits for 1% and 2% of labeled scenes over KITTI train split, We put the proposed theoretical approach into practice. In KITTI, the detection target are divided in hard, moderate and easy 3 levels by the ease of testing, in order to make a comprehensive comparison with the methods that have emerged in recent years, we use cars, pedestrians and cyclists' mean Average Precision (mAP) with 40 recall positions obtained at 0.7, 0.5, and 0.5 3D IoU threshold respectively as the comparative indicators.

**Implementation Details.** In SSF3D, all the model basic setting are same as PV-RCNN [7] from OpenPCDet [42], meanwhile weak augmentation and the EMA momentum factors are also same as prior works [13], [19]. Before the first epoch and each 5 epochs, teacher model will calculate dataset offline to generate pseudo labels as gt database to implement gt sample data-augmentation for further training.

For GMM3 Picker, we set a minimal threshold value for cyclist and pedestrian categories because both of them have a low initial accuracy and lack of data in KITTI dataset, this minimal threshold is set from the final value obtained by the GMM3 Picker method after one stage training without minimal threshold. Meanwhile we use moderate GMM3 thresholds for cyclist and pedestrian categories' filters to ensure the model can reach more pseudo labels. For Dense Loss, we set  $\gamma$  as 2. In second stage of SSF3D, we start our training from a well performed checkpoint from stage-1 80 epochs training, entropy filter's layer length  $l$  is set as 0.06m, and the entropy threshold in 3 dimensions for car category is set as 0.9 after observation from Fig. 5 (a), while for pedestrian and cyclist we didn't change their filter due to random normal variation of small target. One NVIDIA GTX3090 is used for all the training.

### B. Main Results

We evaluated several recent methods on the KITTI dataset and their results are summarized in Tab. I. It is evident that

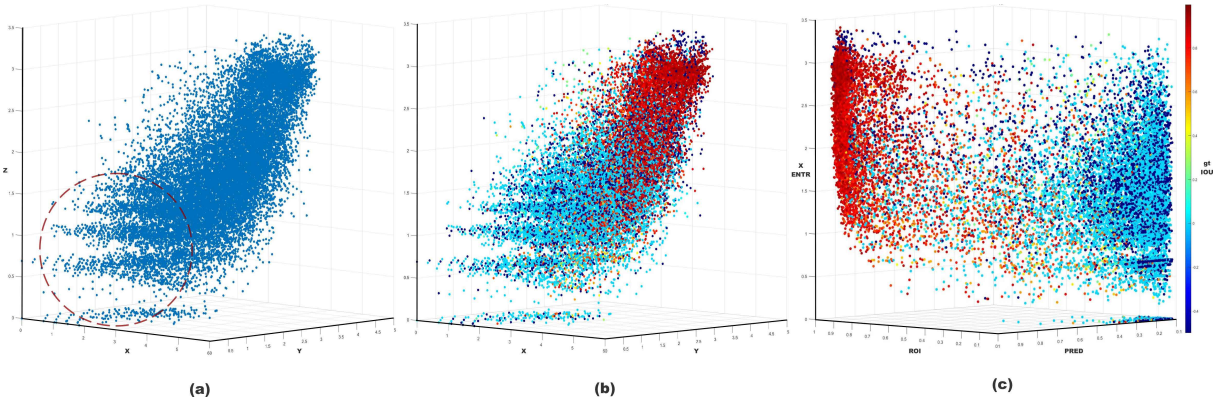


Fig. 5. **Scatterplot of all prediction boxes.** Each points in the scatterplot represents a 1-stage-trained teacher model prediction box. The darker the red color, the higher the  $IOU_{gt}$ , and the dark blue indicates a classification error. (a) The scatterplot of entropy score in target's x,y,z dimension. (b) same scatterplot as Fig.(a) but with  $IOU_{gt}$  color. (c) The scatterplot of confidence, roi and x-axis entropy score with  $IOU_{gt}$  color.

Model	1%				2%			
	Car	Ped.	Cyc.	Avg.	Car	Ped.	Cyc.	Avg.
PV-RCNN [7]	73.5	28.7	28.4	43.5	76.6	40.8	45.5	54.3
3DIOUMatch [19]	76.0	31.7	36.4	48.0	78.7	48.2	56.2	61.0
3DDSD [36]	76.0	34.8	38.5	49.7	78.9	49.4	53.9	60.7
DetMatch [25]	77.5	<b>57.3</b>	42.3	59.0	78.2	54.1	64.7	65.6
HSSDA [13]	80.9	51.9	45.7	59.5	81.9	58.2	65.8	68.6
Our SSF3D	<b>83.4</b>	54.3	<b>65.6</b>	<b>67.7</b>	<b>84.7</b>	<b>58.6</b>	<b>71.1</b>	<b>71.4</b>

TABLE I

COMPARISONS WERE MADE BETWEEN OUR EXPERIMENTAL FINDINGS ON THE KITTI DATASET AND THE MOST RECENT STATE-OF-THE-ART METHODS. THESE RESULTS WERE DOCUMENTED ACROSS 40 RECALL POSITIONS, EMPLOYING IOU THRESHOLDS OF 0.7, 0.5, AND 0.5 FOR 'CAR', 'PEDESTRIAN', AND 'CYCLIST', RESPECTIVELY.

Model	Car			Pedestrian			Cyclist		
	Easy	Mod	Hard	Easy	Mod	Hard	Easy	Mod	Hard
Voxel-RCNN*	88.08	76.15	71.58	47.40	42.18	37.35	62.55	44.74	41.30
HSSDA*	90.26	76.76	71.57	57.74	49.65	43.49	<b>73.24</b>	51.82	48.71
SDF3D	<b>90.54</b>	<b>79.70</b>	<b>74.96</b>	<b>60.84</b>	<b>53.77</b>	<b>47.52</b>	71.18	<b>52.92</b>	<b>49.35</b>

TABLE II

RESULTS COMPARISON ON THE KITTI DATASET USING THE VOXEL-RCNN DETECTOR AS TEST BED, USED 100 EPOCHS TRAINING, USED 2% LABEL DATASET, METRICS ARE SAME AS TABLE I. \* MEANS REPRODUCED BY US.

SSF3D consistently achieves high accuracy across various initial labeled dataset splits. In concrete terms, our approach significantly enhanced model performance, the average mAP have a remarkable increase of nearly 8% and 5% for annotation splits of 1% and 2%, respectively. The results of full-labeled PV-RCNN from the PCDet provided checkpoint are also included in the Tab. III. We consider that for pedestrian and cyclist categories, the reason why the performance of SSF3D and several previous works better than full-dataset result are similar, is that these semi-supervised methods filter out some ambiguous labels in the initial.

At the same time, we used Voxel-RCNN [40] as a test and placed the results in Table II to demonstrate the portability of our method for any other LIDAR point cloud based algorithm. We reproduced all the experiments with a mini-batch as 2 for adapting our GPU memory, and the results show that SSF3D still have a improvement over the state-of-the-art methods.

### C. Ablation Study

All the experiments in this Section are tested on the 2% KITTI dataset, same metric as Tab. I, and the total ablation test form is shown in Tab. III.

**Effect of GMM3 Picker.** The GMM3 Picker is used during both stage, while the threshold changing curve can be seen in Fig. 2. As shown in Tab. III Exp. 2, after a suitable threshold have been choice, detection mAP improved by 2% in the cars category and 7% in the cycles category.

We also set up some comparative experiments to prove the influence of different threshold selection on the model accuracy. As shown in the Tab. IV, compare to HSSDA, who also use a point remove strategy and automatically threshold picking, we generate more strict but not extreme threshold and get a better result. At the same time, Tab. IV proves that too high and too low thresholds are meaningless even for the method with a point remove strategy.

**Effect of Dense Loss.** Dense loss is also used in all stage in SSF3D, from Tab. III Exp. 3, it can be seen that this function played an auxiliary role in strict semi-supervision mechanism. It does not bring as great an effect as the GMM3 Picker, but it also has a positive effect.

**Effect of Entropy Filter.** Entropy Filter is used in the second stage of SSF3D, as Tab. III Exp. 4, after 40 epochs Stage-2 training, the car category has a boost with 2% increase in the hard level object. While pedestrian and cyclist categories both have some minor fluctuations, we believe this results from the fact that the point normals of small targets vary dramatically, making their information entropy ineffective in identifying the validity of some of the prediction frames. Meanwhile the initial labels of pedestrian and cyclist categories are very few, thus there are few fuzzy semantic labels need to filter by entropy filter. Therefore in the main structure of SSF3D, we did not implement filter changes for cyclist and pedestrian, only on the car category.

Further, we conduct some experiments for the selection of the entropy thresholds, and the results are shown in Tab. V, according to the results, the entropy filter in z-axis has the most

	GMM	DSL	ENF	Easy	Car Mod	Hard	Easy	Ped. Mod	Hard	Easy	Cyc. Mod	Hard
Exp.1	-	-	-	91.36	79.53	74.63	57.86	51.84	46.72	79.37	61.04	57.24
Exp.2	✓	-	-	92.29	81.77	77.38	65.89	58.21	52.01	90.43	65.93	62.05
Exp.3	✓	✓	-	93.09	82.18	77.42	<b>66.27</b>	<b>58.35</b>	<b>52.24</b>	<b>91.58</b>	<b>66.31</b>	<b>62.87</b>
Exp.4	✓	✓	✓	<b>93.12</b>	<b>82.48</b>	<b>79.38</b>	64.38	56.02	49.35	90.66	66.24	62.43
100% labled	-	-	-	91.38	82.86	81.92	62.43	53.17	48.44	87.89	69.71	65.53

TABLE III

"GMM" MEANS GMM3 PICKER MODULE, "DSL" MEANS DENSE LOSS AND "ENF" MEANS FILTER CHANGE WITH ENTROPY FILTER. ACCORDING TO THE RESULTS OF THIS TABLE, WE CONDUCT SWITCH OF ENTROPY FILTER ONLY ON CAR CATEGORY.

threshold	con	roi	cus	Car
fixed high	0.99	0.97	0.9	79.6
fixed low	0.5	0.5	0.5	76.7
HSSDA [13]	0.41	0.42	0.91	81.9
GMM3(our)	0.96	0.91	0.88	<b>83.3</b>

TABLE IV

**THE EFFECT OF DIFFERENT THRESHOLD SELECTION ON THE MODEL ACCURACY.** FOR CAR CATEGORY, WE LIST THE FIRST EPOCH'S THREE THRESHOLDS AND THE FINAL AVERAGE MAP SCORE OF THE MODEL, THESE THRESHOLD REPRESENT THE LOWEST SCORE OF A LABEL THAT CAN BE LEARNED BY THE MODEL; "CON" MEANS CONFIDENCE SCORE, "ROI" MEANS ROI SCORE AND "CUS" MEANS CUSTOM FILTER SCORE.

entr_x	entr_y	entr_z	Car_easy	Car_mid	Car_hard
1.0	0	0	93.02	82.37	78.72
0	1.0	0	1	1	1
0	0	0.9	92.59	82.39	79.29
1.0	1.0	0.9	93.12	82.48	79.38

TABLE V

**COMPARISON OF ENTROPY FILTERS APPLIED ON DIFFERENT AXES.** WE APPLY ENTROPY FILTER ON DIFFERENT AXES AND THE RESULT IS SHOWN IN THE TABLE.

significant impact on the model's performance, we consider that this is because most of ambiguous labels have a low entropy score in z-axis. For example, the point cloud z-axis distribution of a distant target will naturally be more sparse than a near target, and it will have a higher probability of return noise with occlusion.

Information entropy as a filtering lacks of filtering accuracy compared to IOU filters designed based on confidence scores, but it is sufficient to filter out ambiguous targets that are difficult to distinguish from the model's own judgment, what's more, the latent distribution of pseudo labels is also slightly changed by filter switching.

## V. CONCLUSION

In this paper, we have made a series of explorations in the SS3DOD training framework and proposed a two-stage training architecture: SSF3D. In both stages GMM3 Picker and Dense Loss has been introduced to conduct a semi-supervised training with fewer interference from false-negative/positive labels. In Stage 2 a new filter has been introduced to obtain different distribution objects as labels, meanwhile filter out ambiguous labels which have lower information entropy.

The experiments confirm that the architecture of deleting and adding is effective, deleting noise points in low score labels eliminated disturb from false-negative labels and adding high score labels from the pseudo labels database keeps the

complexity of scenes. Based on this architecture, conduct a strict filter of pseudo labels significantly improved the model's performance, and GMM3 Picker, Dense Loss, Entropy filter proposed in this paper can helpfully achieve this goal.

## REFERENCES

- [1] X. Yang, Z. Song, I. King, and Z. Xu, "A survey on deep semi-supervised learning," *IEEE Transactions on Knowledge and Data Engineering*, 2022.
- [2] C. Hu, X. Li, D. Liu, X. Chen, J. Wang, and X. Liu, "Teacher-student architecture for knowledge learning: A survey," *arXiv preprint arXiv:2210.17332*, 2022.
- [3] W. Zheng, W. Tang, S. Chen, L. Jiang, and C.-W. Fu, "Cia-ssd: Confident iou-aware single-stage object detector from point cloud," in *Proceedings of the AAAI conference on artificial intelligence*, vol. 35, no. 4, 2021, pp. 3555–3562.
- [4] L. Fan, Z. Pang, T. Zhang, Y.-X. Wang, H. Zhao, F. Wang, N. Wang, and Z. Zhang, "Embracing single stride 3d object detector with sparse transformer," in *Proceedings of the IEEE/CVF conference on computer vision and pattern recognition*, 2022, pp. 8458–8468.
- [5] A. H. Lang, S. Vora, H. Caesar, L. Zhou, J. Yang, and O. Beijbom, "Pointpillars: Fast encoders for object detection from point clouds," in *Proceedings of the IEEE/CVF conference on computer vision and pattern recognition*, 2019, pp. 12 697–12 705.
- [6] J. Li, C. Luo, and X. Yang, "Pillarnext: Rethinking network designs for 3d object detection in lidar point clouds," in *Proceedings of the IEEE/CVF Conference on Computer Vision and Pattern Recognition*, 2023, pp. 17 567–17 576.
- [7] S. Shi, C. Guo, L. Jiang, Z. Wang, J. Shi, X. Wang, and H. Li, "Pv-rccn: Point-voxel feature set abstraction for 3d object detection," in *Proceedings of the IEEE/CVF conference on computer vision and pattern recognition*, 2020, pp. 10 529–10 538.
- [8] S. Shi, L. Jiang, J. Deng, Z. Wang, C. Guo, J. Shi, X. Wang, and H. Li, "Pv-rccn++: Point-voxel feature set abstraction with local vector representation for 3d object detection," *International Journal of Computer Vision*, vol. 131, no. 2, pp. 531–551, 2023.
- [9] T. Yin, X. Zhou, and P. Krahenbuhl, "Center-based 3d object detection and tracking," in *Proceedings of the IEEE/CVF conference on computer vision and pattern recognition*, 2021, pp. 11 784–11 793.
- [10] T. Liang, H. Xie, K. Yu, Z. Xia, Z. Lin, Y. Wang, T. Tang, B. Wang, and Z. Tang, "Befusion: A simple and robust lidar-camera fusion framework," *Advances in Neural Information Processing Systems*, vol. 35, pp. 10 421–10 434, 2022.
- [11] Z. Liu, X. Ye, Z. Zou, X. He, X. Tan, E. Ding, J. Wang, and X. Bai, "Multi-modal 3d object detection by box matching," *arXiv preprint arXiv:2305.07713*, 2023.
- [12] B. Chen, W. Chen, S. Yang, Y. Xuan, J. Song, D. Xie, S. Pu, M. Song, and Y. Zhuang, "Label matching semi-supervised object detection," in *Proceedings of the IEEE/CVF Conference on Computer Vision and Pattern Recognition*, 2022, pp. 14 381–14 390.
- [13] C. Liu, C. Gao, F. Liu, P. Li, D. Meng, and X. Gao, "Hierarchical supervision and shuffle data augmentation for 3d semi-supervised object detection," in *Proceedings of the IEEE/CVF Conference on Computer Vision and Pattern Recognition*, 2023, pp. 23 819–23 828.
- [14] X. Wang, X. Yang, S. Zhang, Y. Li, L. Feng, S. Fang, C. Lyu, K. Chen, and W. Zhang, "Consistent-teacher: Towards reducing inconsistent pseudo-targets in semi-supervised object detection," in *Proceedings of the IEEE/CVF Conference on Computer Vision and Pattern Recognition*, 2023, pp. 3240–3249.

- [15] M. Xu, Z. Zhang, H. Hu, J. Wang, L. Wang, F. Wei, X. Bai, and Z. Liu, "End-to-end semi-supervised object detection with soft teacher," in *Proceedings of the IEEE/CVF International Conference on Computer Vision*, 2021, pp. 3060–3069.
- [16] H. Zhou, Z. Ge, S. Liu, W. Mao, Z. Li, H. Yu, and J. Sun, "Dense teacher: Dense pseudo-labels for semi-supervised object detection," in *European Conference on Computer Vision*. Springer, 2022, pp. 35–50.
- [17] C.-J. Ho, C.-H. Tai, Y.-H. Tsai, Y.-Y. Lin, and M.-H. Yang, "Learning Object-level Point Augmentor for Semi-supervised 3D Object Detection," Dec. 2022.
- [18] J. Li, Z. Liu, J. Hou, and D. Liang, "Dds3d: Dense pseudo-labels with dynamic threshold for semi-supervised 3d object detection," *arXiv preprint arXiv:2303.05079*, 2023.
- [19] H. Wang, Y. Cong, O. Litany, Y. Gao, and L. J. Guibas, "3dioumatch: Leveraging iou prediction for semi-supervised 3d object detection," in *Proceedings of the IEEE/CVF Conference on Computer Vision and Pattern Recognition*, 2021, pp. 14 615–14 624.
- [20] Y.-C. Liu, C.-Y. Ma, Z. He, C.-W. Kuo, K. Chen, P. Zhang, B. Wu, Z. Kira, and P. Vajda, "Unbiased teacher for semi-supervised object detection," *arXiv preprint arXiv:2102.09480*, 2021.
- [21] K. Sohn, Z. Zhang, C.-L. Li, H. Zhang, C.-Y. Lee, and T. Pfister, "A simple semi-supervised learning framework for object detection," *arXiv preprint arXiv:2005.04757*, 2020.
- [22] Q. Xie, Z. Dai, E. Hovy, T. Luong, and Q. Le, "Unsupervised data augmentation for consistency training," *Advances in neural information processing systems*, vol. 33, pp. 6256–6268, 2020.
- [23] W. Zheng, W. Tang, L. Jiang, and C.-W. Fu, "Se-ssd: Self-ensembling single-stage object detector from point cloud," in *Proceedings of the IEEE/CVF Conference on Computer Vision and Pattern Recognition*, 2021, pp. 14 494–14 503.
- [24] Y. Yan, Y. Mao, and B. Li, "Second: Sparsely embedded convolutional detection," *Sensors*, vol. 18, no. 10, 2018. [Online]. Available: <https://www.mdpi.com/1424-8220/18/10/3337>
- [25] J. Park, C. Xu, Y. Zhou, M. Tomizuka, and W. Zhan, "Detmatch: Two teachers are better than one for joint 2d and 3d semi-supervised object detection," in *European Conference on Computer Vision*. Springer, 2022, pp. 370–389.
- [26] Y. Chen, V. T. Hu, E. Gavves, T. Mensink, P. Mettes, P. Yang, and C. G. Snoek, "Pointmixup: Augmentation for point clouds," in *Computer Vision—ECCV 2020: 16th European Conference, Glasgow, UK, August 23–28, 2020, Proceedings, Part III 16*. Springer, 2020, pp. 330–345.
- [27] M. Hong, J. Choi, and G. Kim, "StyleMix: Separating Content and Style for Enhanced Data Augmentation," in *2021 IEEE/CVF Conference on Computer Vision and Pattern Recognition (CVPR)*. Nashville, TN, USA: IEEE, Jun. 2021, pp. 14 857–14 865.
- [28] S. Yun, D. Han, S. J. Oh, S. Chun, J. Choe, and Y. Yoo, "Cutmix: Regularization strategy to train strong classifiers with localizable features," in *Proceedings of the IEEE/CVF international conference on computer vision*, 2019, pp. 6023–6032.
- [29] N. Zhao, T.-S. Chua, and G. H. Lee, "Sess: Self-ensembling semi-supervised 3d object detection," in *Proceedings of the IEEE/CVF Conference on Computer Vision and Pattern Recognition*, 2020, pp. 11 079–11 087.
- [30] Y.-C. Liu, C.-Y. Ma, and Z. Kira, "Unbiased teacher v2: Semi-supervised object detection for anchor-free and anchor-based detectors," in *Proceedings of the IEEE/CVF Conference on Computer Vision and Pattern Recognition*, 2022, pp. 9819–9828.
- [31] T.-Y. Lin, P. Goyal, R. Girshick, K. He, and P. Dollár, "Focal loss for dense object detection," in *Proceedings of the IEEE international conference on computer vision*, 2017, pp. 2980–2988.
- [32] A. Geiger, P. Lenz, C. Stiller, and R. Urtasun, "Vision meets robotics: The KITTI dataset," *The International Journal of Robotics Research*, vol. 32, no. 11, pp. 1231–1237, Sep. 2013.
- [33] S. Shi, Z. Wang, J. Shi, X. Wang, and H. Li, "From points to parts: 3d object detection from point cloud with part-aware and part-aggregation network," *IEEE transactions on pattern analysis and machine intelligence*, vol. 43, no. 8, pp. 2647–2664, 2020.
- [34] Z. Zhou, X. Zhao, Y. Wang, P. Wang, and H. Foroosh, "Centerformer: Center-based transformer for 3d object detection," in *European Conference on Computer Vision*. Springer, 2022, pp. 496–513.
- [35] C. R. Qi, O. Litany, K. He, and L. J. Guibas, "Deep hough voting for 3d object detection in point clouds," in *proceedings of the IEEE/CVF International Conference on Computer Vision*, 2019, pp. 9277–9286.
- [36] Z. Yang, Y. Sun, S. Liu, and J. Jia, "3dssd: Point-based 3d single stage object detector," in *Proceedings of the IEEE/CVF conference on computer vision and pattern recognition*, 2020, pp. 11 040–11 048.
- [37] M. Xu, R. Ding, H. Zhao, and X. Qi, "Paconv: Position adaptive convolution with dynamic kernel assembling on point clouds," in *Proceedings of the IEEE/CVF Conference on Computer Vision and Pattern Recognition*, 2021, pp. 3173–3182.
- [38] S. Shi, X. Wang, and H. Li, "Pointcnn: 3d object proposal generation and detection from point cloud," in *Proceedings of the IEEE/CVF conference on computer vision and pattern recognition*, 2019, pp. 770–779.
- [39] C. He, H. Zeng, J. Huang, X.-S. Hua, and L. Zhang, "Structure aware single-stage 3d object detection from point cloud," in *Proceedings of the IEEE/CVF conference on computer vision and pattern recognition*, 2020, pp. 11 873–11 882.
- [40] J. Deng, S. Shi, P. Li, W. Zhou, Y. Zhang, and H. Li, "Voxel r-cnn: Towards high performance voxel-based 3d object detection," in *Proceedings of the AAAI Conference on Artificial Intelligence*, vol. 35, no. 2, 2021, pp. 1201–1209.
- [41] A. Vaswani, N. Shazeer, N. Parmar, J. Uszkoreit, L. Jones, A. N. Gomez, Ł. Kaiser, and I. Polosukhin, "Attention is all you need," *Advances in neural information processing systems*, vol. 30, 2017.
- [42] O. D. Team, "Openpcdet: An open-source toolbox for 3d object detection from point clouds," <https://github.com/open-mmlab/OpenPCDet>, 2020.
- [43] R. B. Rusu, N. Blodow, and M. Beetz, "Fast point feature histograms (fpfh) for 3d registration," in *2009 IEEE International Conference on Robotics and Automation*, 2009, pp. 3212–3217.
- [44] F. Tombari, S. Salti, and L. Di Stefano, "Unique signatures of histograms for local surface description," in *Computer Vision – ECCV 2010*, K. Daniilidis, P. Maragos, and N. Paragios, Eds. Berlin, Heidelberg: Springer Berlin Heidelberg, 2010, pp. 356–369.
- [45] R. B. Rusu, N. Blodow, Z. C. Marton, and M. Beetz, "Aligning point cloud views using persistent feature histograms," in *2008 IEEE/RSJ International Conference on Intelligent Robots and Systems*, 2008, pp. 3384–3391.